Archives of Biochemistry and Biophysics 604 (2016) 167–176

Contents lists available at ScienceDirect

Archives of Biochemistry and Biophysics

journal homepage: www.elsevier.com/locate/yabbi

Antibacterial properties and mechanism of graphene oxide-silver nanocomposites as bactericidal agents for water disinfection

Biao Song [a, b], Chang Zhang [a, b], Guangming Zeng [a, b, *], Jilai Gong [a, b, **], Yingna Chang [a, b], Yan Jiang [a, b]

[a] College of Environmental Science and Engineering, Hunan University, Changsha 410082, PR China
[b] Key Laboratory of Environmental Biology and Pollution Control (Hunan University), Ministry of Education, Changsha 410082, PR China

ARTICLE INFO

Article history:
Received 7 April 2016
Received in revised form
26 April 2016
Accepted 28 April 2016
Available online 8 May 2016

Keywords:
Graphene oxide
Silver nanoparticles
Antibacterial
Water disinfection

ABSTRACT

Providing clean and affordable drinking water without harmful disinfection byproducts generated by conventional chemical disinfectants gives rise to the need for technological innovation. Nanotechnology has great potential in purifying water and wastewater treatment. A graphene oxide-silver (GO-Ag) nanocomposite with excellent antibacterial activity was prepared and characterized by transmission electron microscope and X-ray photoelectron spectroscopy. The tests were carried out using *Escherichia coli* and *Staphylococcus aureus* as model strains of Gram-negative and Gram-positive bacteria, respectively. The effect of bactericide dosage and pH on antibacterial activity of GO-Ag was examined. Morphological observation of bacterial cells by scanning electron microscope showed that GO-Ag was much more destructive to cell membrane of *Escherichia coli* than that of *Staphylococcus aureus*. Experiments were carried out using catalase, superoxide dismutase and sodium thioglycollate to investigate the formation of reactive oxygen species and free silver ions in the bactericidal process. The activity of intracellular antioxidant enzymes was measured to investigate the potential role of oxidative stress. According to the consequence, synergetic mechanism including destruction of cell membranes and oxidative stress accounted for the antibacterial activity of GO-Ag nanocomposites. All the results suggested that GO-Ag nanocomposites displayed a good potential for application in water disinfection.

1. Introduction

Disinfection of pathogenic microorganisms is an essential process of supplying safe potable water from public water system. Chlorine [1], chlorine dioxide [2], ozone [3], and chloramines [4] are the most common disinfectants in use today. Although these disinfectants can effectively kill microbial pathogens, they can also oxide anthropogenic contaminants, organic matter naturally present in source waters due to their strong oxidizing property, which leads to the formation of disinfection by-products (DBPs) [5], such as trihalomethanes (THMs) [6], haloacetic acids (HAAs) [7], bromate [8] and chlorite [9], the well-known teratogens and carcinogens. Therefore, the demand of developing new generations of antimicrobial agents for effectively killing pathogenic bacteria in drinking water is becoming crucial.

Silver and silver compounds exhibit a strong antibacterial activity to a wide range of microorganisms, including *Pseudomonas aeruginosa*, *Escherichia coli (E. coli)*, *Staphylococcus aureus (S. aureus)* and *Candida albicans* [10,11]. Nano-silver is a relatively new and different type of silver with different chemical and physical properties. Silver nanoparticles (AgNPs) show much better antibacterial activity compared with conventional silver-based bactericide [12]. However, the mechanism of antibacterial effect of AgNPs remains not fully understood.

Graphene oxide (GO), a monolayer of carbon atoms that form dense honeycomb structures containing hydroxyl and epoxide functional groups on the two sides and carboxylic groups at the edges, is often used to load metal nanoparticles as these nanoparticles tend to aggregate to minimize their surface energy in the process of preparation [13]. Additionally, it has been proved that GO exhibit antibacterial activity against many bacterial species [14,15]. Hence, the introduction of AgNPs onto GO can not only solve the

* Corresponding author. College of Environmental Science and Engineering, Hunan University, Changsha 410082, PR China.
** Corresponding author. College of Environmental Science and Engineering, Hunan University, Changsha 410082, PR China.
E-mail addresses: zgming@hnu.edu.cn (G. Zeng), jilaigong@gmail.com (J. Gong).

http://dx.doi.org/10.1016/j.abb.2016.04.018
0003-9861/

problem of aggregation and stability of AgNPs, but also combine the bactericidal effect of GO and AgNPs. Although many researchers has reported Ag loaded on GO sheets for laboratory and medical devices disinfection [16], purification of fuel and non-polar solvents [17], and food packaging [18], the bactericidal process were both conducted in a static state with agar diffusion method and evaluated by the inhibition zone in these studies. In our tests, the interaction between bactericide and bacteria was carried out in aqueous solution with moderate stirring. Recently, many nanomaterials, such as AgNPs@chitosan-TiO_2 [19], palladium incorporated ZnO [20], silica-silver nanocomposites [21], and iron oxide magnetic nanoparticles [22], were explored as disinfectants for drinking water treatment, but, to our knowledge, the use of silver nanoparticles loaded on GO sheets as bactericides for water disinfection was rare. Compared with AgNPs@chitosan-TiO_2 and palladium incorporated ZnO, the disinfection using silver nanoparticles loaded on GO sheets did not need optical radiation for photocatalysis. And the distribution of silver nanoparticles were more homogeneous with GO than silica-silver nanocomposites and iron oxide magnetic nanoparticles.

In this work, we synthesized graphene oxide-silver (GO-Ag) nanocomposites and used it as bactericide for drinking water disinfection. Gram-positive bacteria, *S. aureus*, and Gram-negative bacteria, *E. coli*, were selected as models to investigate the antimicrobial properties of the composites towards different species of bacteria. Antibacterial activity under different conditions including different bactericide dosage and pH was investigated. The antibacterial mechanism of GO-Ag was also explored by morphological observation, bactericidal species and bactericidal process analysis.

2. Materials and methods

2.1. Materials

Graphite powders were obtained from Jin-Shan-Ting New Chemical Factory (Shanghai, China). Sodium nitrate ($NaNO_3$), sulfuric acid (H_2SO_4, 98%), potassium permanganate ($KMnO_4$), hydrogen peroxide (H_2O_2, 30%), and absolute ethanol (CH_3CH_2OH) were purchased from Sinopharm Chemical Reagent Company (Shanghai, China). Silver nitrate ($AgNO_3$) was supplied by Beijing Chemical Factory (Beijing, China). Ammonium formate ($HCOONH_4$) was obtained from Kermel Chemical Reagent Company (Tianjin, China). Catalase (CAT), superoxide dismutase (SOD) and sodium thioglycollate (NATG) were purchased from Xiya Chemical Industry Company (Shandong, China). All chemicals in this study were analytical grade and were used as received without any further purification.

The strains employed in this work were the Gram-negative bacterium *E. coli* (ATCC 25922) and the Gram-positive bacterium *S. aureus* (ATCC 6538), which were purchased from the China Center for Type Culture Collection (Wuhan, China).

2.2. Preparation of GO suspension

GO was prepared from powder graphite by adopting modified Hummer and Offeman method [23,24]. Concretely, 1 g graphite powders, 0.5 g $NaNO_3$ and 23 mL concentrated H_2SO_4 were added into a 1 L beaker flask. Under ice bath and stirring condition, 3 g $KMnO_4$ was added slowly. The reaction was continued at a constant temperature of 35 °C with stirring for 30 min, followed by dilution with 46 mL warm de-ionized (DI) water. Subsequently, the reaction temperature was increased to 98 °C for another 30 min with stirring, and then reaction mixture was diluted by 140 mL DI water and the residual permanganate and manganese dioxide were reduced by adding 2.5 mL H_2O_2 with a change of suspension color from brown to yellow. The resulting suspension was centrifuged to collect solid product which was washed with absolute ethanol and DI water sequentially until the pH of the supernatant reached 7. Afterwards, the product was dried in a vacuum oven to obtain graphite oxide powders. Finally, homogeneous GO suspension in reddish brown was obtained through ultrasonic exfoliation of the graphite oxide dispersed in DI water for 1 h.

2.3. Preparation of GO-Ag

GO-Ag nanocomposites were prepared by reducing $AgNO_3$ with $HCOONH_4$ in presence of GO suspension [25]. Briefly, 0.4 g $AgNO_3$ was added into GO suspension pre-prepared from 0.5 g GO and mixed it uniformly. After that, 50 mL 0.5 mol L^{-1} $HCOONH_4$ aqueous solution was added drop by drop with stirring at room temperature for 1 h to induce complete reduction. After 24 h ageing, the mixture was centrifuged and washed with absolute ethanol and DI water sequentially. Then, GO-Ag nanocomposites were obtained after drying in a vacuum oven for 12 h.

2.4. Characterization

The sizes and morphologies of GO and GO-Ag were characterized by transmission electron microscopy (TEM) (JEOL-1230 microscope, Japan). The composition and bond energy information of GO and GO-Ag were investigated by X-ray photoelectron spectroscopy (XPS) (K-Alpha 1063, United Kingdom) using a Thermo Fisher Scientific Theta Probe Spectrometer equipped with Al Kα Micro gathered monochromator as the source of X-ray. Binding energy of Ag was measured by referring to the C 1s peak at 284.8 eV. Detailed spectra processing was performed by commercial Thermo Avantage software (v. 5.52, ©1999–2012 Thermo Fisher Scientific Inc.).

2.5. Bacterial culture and counting method

The bacterial strains were cultivated in Luria-Bertani (LB) fluid nutrient medium (tryptone 10 g L^{-1}, yeast extract 5 g L^{-1}, and NaCl 5 g L^{-1}) with approximately 120 rpm shaking speed at 37 °C for 24 h. Then, bacterial cells were gathered by centrifugation and washed three times to remove all residual LB. Finally, the bacterial cells were re-suspended in sterile water and diluted to achieve the desired initial concentrations containing cells 10^5–10^6 CFU mL^{-1}. All experimental mediums and glass wares were sterilized at 121 °C for 15 min with autoclave before they were used.

The antibacterial activity of GO-Ag and the microbial changes were evaluated by plate colony-counting method. Concretely, the undetermined samples were diluted by ten times gradient dilution with sterile water. After that, for the purpose of inhibiting other microorganisms and forming uniform colonies, 100 μL of each test sample was spread on a selective eosin methylene blue agar plate (for *E. coli*) or mannitol salt agar plate (for *S. aureus*), followed by cultivation at 37 °C for 24 h. Then the number of colonies on the agar plate was counted and recorded for the determination of live bacteria.

The detection limit of this method is 10 CFU mL^{-1}. Antibacterial rate was calculated using the following equation:

$$\text{Antibacterial rate}(\%) = (1 - N_t/N_0) \times 100\% \quad (1)$$

where N_0 is the initial number of bacterial colonies before each experiment and N_t is the instant colony-forming units in the sample at time t after interaction with bactericidal materials.

2.6. Antibacterial activity assessments

Antibacterial experiment was conducted in 50 mL conical flask containing 25 mL sterile water. Bacterial cells suspension and antibacterial materials were added with stirring at room temperature (25 °C) to ensure complete contact. After a period of time, 100 μL test sample was taken out for plate counting.

2.6.1. Effect of bactericide dosage

To explore the antibacterial activity of GO-Ag against different bacteria and evaluate the proper dosage of bactericide, the bactericidal effect was studied with different concentrations of GO-Ag (40 mg L^{-1}, 120 mg L^{-1}, 200 mg L^{-1} and 280 mg L^{-1}). The contact time was 25 min and samples for counting were taken out every 5 min. Live bacteria in the samples were counted with plate colony-counting method mentioned above.

2.6.2. Effect of pH

To obtain further insight into the antibacterial process, the influence of pH value was studied as follows. Solutions under acidic (pH = 5.5), neutral (pH = 7) and alkaline (pH = 8.5) conditions were used to further assess the effect of pH on bactericidal behavior. The dosage of antibacterial materials was 200 mg L^{-1}. The pH values were adjusted with 0.1 M NaOH and 0.1 M HCl using a pH meter. Samples for counting were taken out after a contact time of 25 min. Live bacteria in the samples were counted with plate colony-counting method mentioned above.

2.7. Antibacterial mechanism studies

2.7.1. Morphological observation of bacterial cells

Bacterial cells of 10^5–10^6 CFU were dispersed in 25 mL sterile water and interacted with 5 mg GO-Ag by stirring for 25 min. Cells untreated were used as control. After that, the cells were collected by centrifugation and washed with normal saline three times, followed by re-suspending in sterile water. And then, cell suspensions were carefully dropped on silicon wafers. 2% glutaraldehyde and 1% osmium tetroxide were used to fix the cells. Then, 30, 50, 70, 80, 90, and 100% ethanol dehydrated bacteria cells with sequential treatments for 15 min. Finally, the dried cells were sputter-coated with gold for scanning electron microscope (SEM) imaging.

2.7.2. Influence of silver ions neutralizer and antioxidant enzymes

A silver ions neutralizer (NATG) and two antioxidant enzymes (CAT and SOD) were used to investigate the effect of silver ion and ROS on the antibacterial activity of GO-Ag. CAT, SOD and NATG were added, respectively, to 0.1% w/v for the results presented below. Samples of 100 μL were taken at 0, 10, 20 and 30 min of contact time for counting.

2.7.3. Determination of intracellular SOD and CAT activity

To investigate the potential role of oxidative stress induced by GO-Ag, SOD and CAT activity in bacterial cells were measured. Original cell extract was obtained by ultrasonication in NaCl solution (0.9%) for five separate periods of 6 s at 70 W according to previous literature [26]. The extract was stored at 4 °C before used for further tests.

SOD activity was measured with hydroxylamine method using a nitrite as a detector of superoxide radicals generated by xanthine and xanthine oxidase in the presence of SOD at an absorbance of 550 nm wavelength [27]. The unit of SOD activity was defined as the amount of the enzyme causing 50% inhibition of the color formation.

CAT activity was measured by colorimetric method according to the decrease of absorbance at 405 nm wavelength due to H_2O_2 consumption [28]. One unit of CAT activity was the amount of the enzyme that decomposed 1 μmol of H_2O_2 per second under experimental conditions.

SOD and CAT assay kits were purchased from Jiancheng Bioengineering Institute (Nanjing, China) and all tests were performed according to the specification provided by the manufacturer.

2.7.4. Lipid peroxidation levels

The content of malonaldehyde (MDA) was determined by thiobarbituric acid (TBA) method measuring the absorbance of thiobarbituric acid reactive substances (TBARS) generated by MDA and TBA at 532 nm wavelength [29]. Briefly, 0.1 mL sample attempting to test was mixed well with 4.1 mL of TBA reagent, followed by incubating in a boiling water bath for 40 min. After cooling, the mixture was centrifuged at 4000 rpm for 10 min. The absorbance of the supernatant was recorded by a UV–visible spectrophotometer (UV-2550, Japan) equipped with UVProbe software to estimate the formation of TBARS and the corresponding levels of MDA were calculated compared with blank sample.

2.8. Statistical analysis

All quantitative data are expressed as the mean ± standard deviation (SD) based on at least three independent experiments. Data were graphed using Origin 8.0 software (OriginLab Corporation, Massachusetts, USA). Microsoft Excel 2010 (Microsoft Corporation, Washington, USA) and SPSS Statistics 22 (IBM Corporation, New York, USA) were used for numerical data processing.

3. Results and discussion

3.1. Characterization

The morphologies of the GO and the synthesized GO-Ag bactericide were obtained by TEM (shown in Fig. 1). It was observed that GO with a layered structure has many wrinkles on its smooth surface (Fig. 1a) and many AgNPs ranging in the diameter of 5–15 nm were evenly anchored on the surface of GO sheets to form GO-Ag nanocomposites (Fig. 1b). These nanocomposites were explored as bactericides for killing bacteria in water.

Fig. 2 presents the XPS spectra of full scans of GO and GO-Ag and an element scan of Ag 3d in the GO-Ag nanocomposites. Compared with the XPS spectra of GO (Fig. 2a), a peak of Ag 3d was detected at the binding energy of 368.45eV (Fig. 2b). In the XPS spectra of element scan, two peaks of Ag 3d located at 368.45 (Ag $3d_{5/2}$) and 374.53 (Ag $3d_{3/2}$) eV were observed, which were in good agreement with the previous literature [30]. According to Liu et al. [31], the Ag $3d_{3/2}$ and Ag $3d_{5/2}$ peaks can be further divided into two different peaks at 374.6, 374.08 eV and 368.6, 368.05 eV, respectively. The peaks at 374.6 and 368.6 eV resulted from metallic silver, which confirmed that silver ions were reduced into metallic silver by $HCOONH_4$ and were successfully loaded onto the GO sheets.

The formation mechanism of GO-Ag nanocomposites can be understood as follows: there are many oxygenic functional groups such as hydroxyl, epoxide, carbonyl and carboxyl on the GO, which provides a large amount of binding sites for silver ions. Positively charged silver ions in the aqueous solution were easily captured by negatively charged GO because of electrostatic interaction [32]. Afterwards, silver ions were reduced in situ by $HCOONH_4$ and AgNPs distributed uniformly on GO sheets, which was in accordance with the TEM image of GO-Ag. Additionally, it has been reported that the reduction process was associated with the formation and decomposition of silver formate at room temperature (Eqs. (2) and (3)) [25]. Moreover, the interaction between AgNPs and GO can attribute to physisorption, electrostatic binding

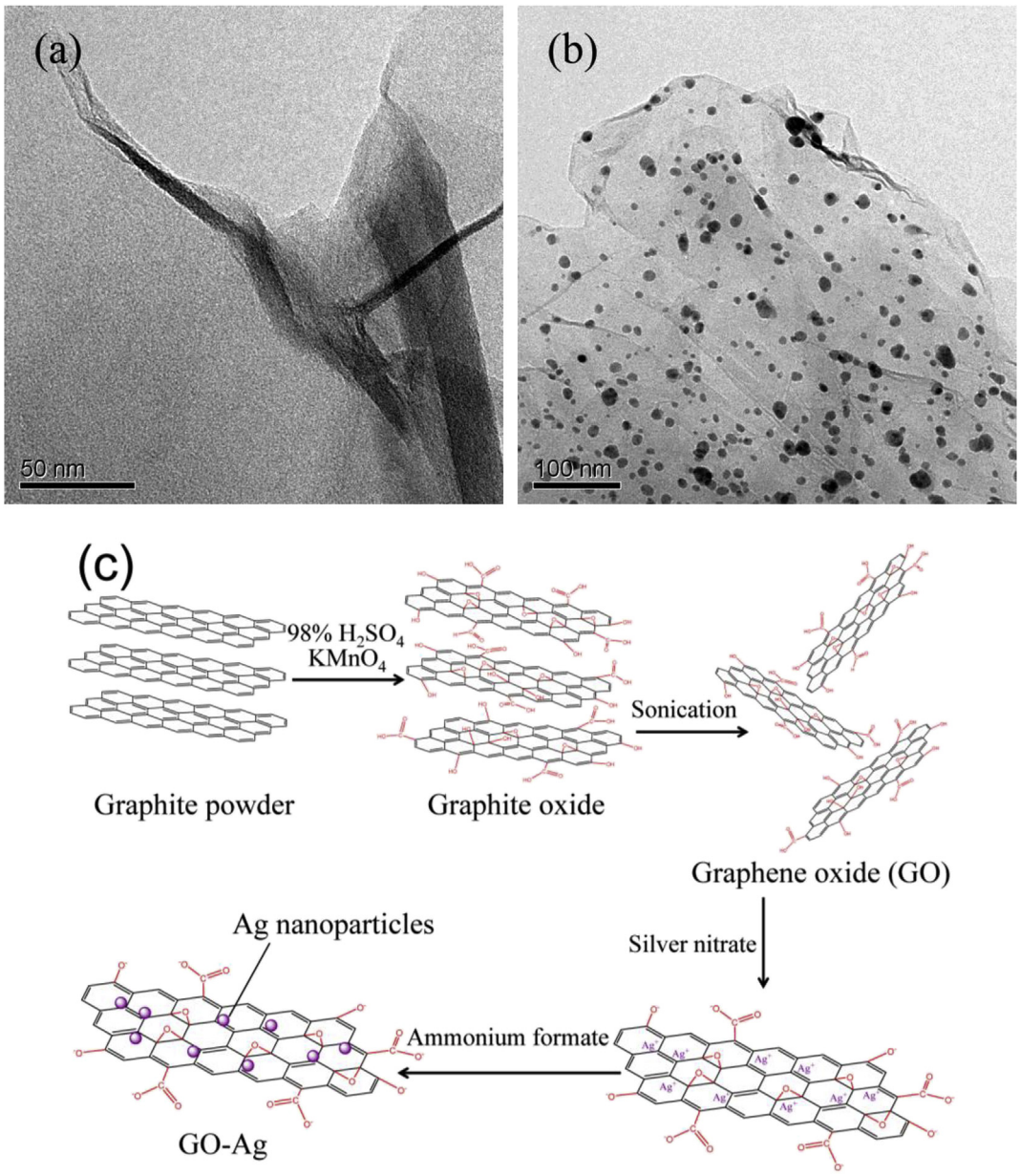

Fig. 1. Transmission electron micrographs of GO (a) and GO-Ag nanocomposites (b), and schematic diagram of GO-Ag synthesis (c).

and charge-transfer interactions as the reduction took place on the surface of GO sheets [33,34]. Thus, a stable GO-Ag nanocomposite was formed and the problem of aggregation and stability of AgNPs was solved. The whole process of GO-Ag synthesis was shown as a diagram (Fig. 1c).

$$AgNO_3 + HCOONH_4 \rightarrow HCOOAg + NH_4^+ + NO_3^- \quad (2)$$

$$HCOOAg \rightarrow Ag + CO_2 + HCOOH \quad (25\ ^\circ C) \quad (3)$$

3.2. Antibacterial activity assessments

3.2.1. Bactericide dosage

The effect of bactericide dosage on the antibacterial activity against *E. coli* and *S. aureus* was illustrated in Fig. 3. When only GO was added, there were a little decrease (3%–5%) of antibacterial activity observed. But our former literature reported that GO exhibited obvious antibacterial activity [24]. The difference lies in the contact time. In this study, for the purpose of obtaining quick and distinct results, the bactericidal process was controlled in 25 min rather than 2 h. And it was found that the antibacterial behavior of GO-Ag against both bacterial strains was not only a dose-dependent process, but also a contact time-dependent one. At 25 min, the antibacterial rates for *E. coli* reached 89.72%, 97.83%, 99.99%, and 99.99%, while the antibacterial rates for *S. aureus* were 70.32%, 95.53%, 95.70% and 97.65%, when the concentrations of GO-Ag were 40, 120, 200 and 280 mg L^{-1}, respectively.

Additionally, it was noticed that the antibacterial activity was more effective against *E. coli* than *S. aureus*. Our comparison experiments showed that when the concentration of GO-Ag was 280 mg L^{-1}, the minimum time were 20 and 30 min for antibacterial rates to reach 99.99% in the tests of *E. coli* and *S. aureus*,

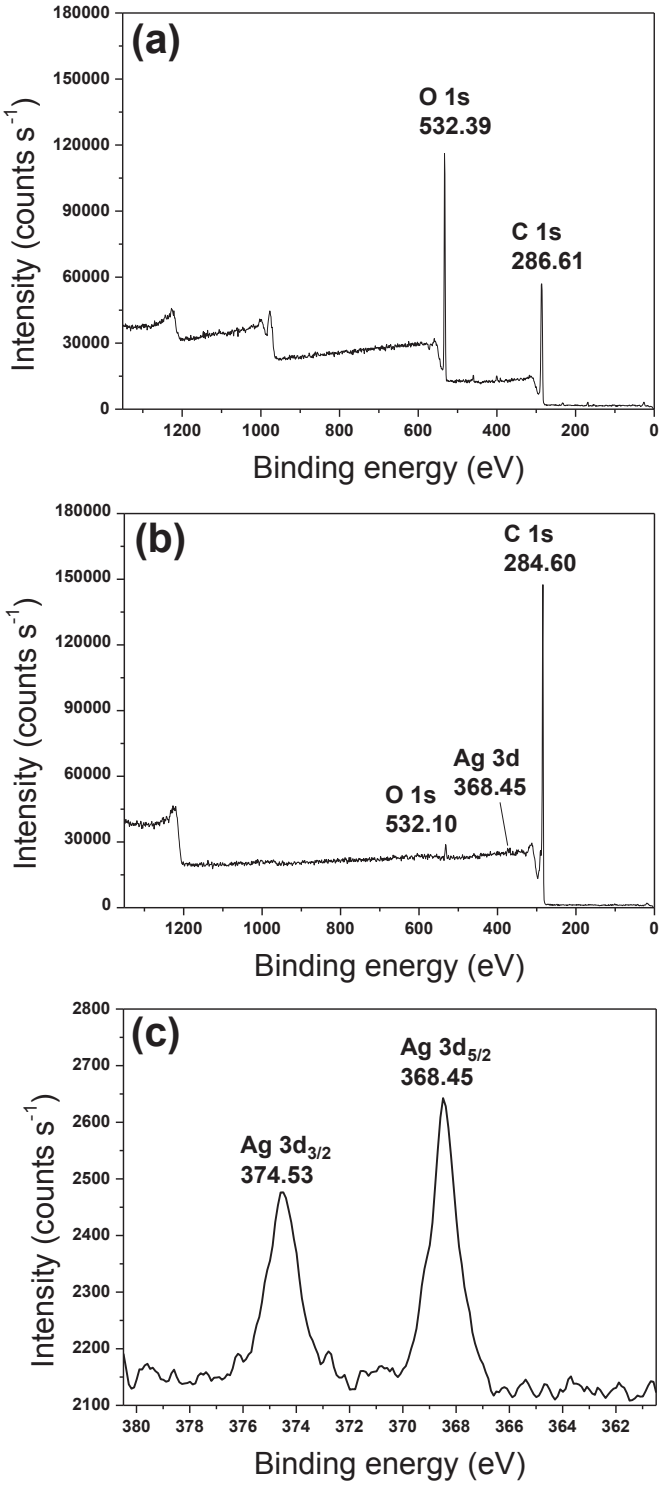

Fig. 2. XPS spectra of GO and GO-Ag composites: full scan of GO (a) and GO-Ag (b), element scan of Ag 3d in the GO-Ag composites (c). Binding energy of Ag was measured by referring to the C 1s peak at 284.6 eV.

respectively. These results are related to the membrane structures of different bacterial species according to previous studies [35]. It was reported that Gram-positive bacteria, *S. aureus*, has thicker cell wall than *E. coli* species. Hence, the reticular structure of peptidoglycan layer in Gram-negative bacteria is looser and exhibits a lower mechanical strength. As a result, the permeation of silver into cells of *S. aureus* species was more difficult.

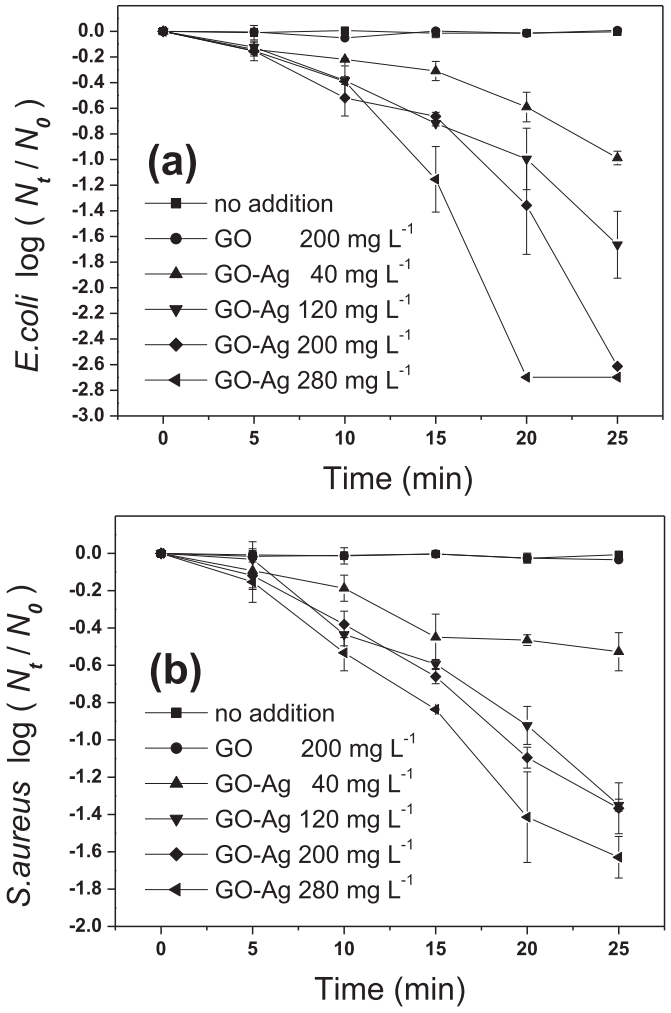

Fig. 3. Effect of bactericide dosage on antibacterial activity against *E. coli* (a) and *S. aureus* (b). The concentrations of GO-Ag were 40, 120, 200, and 280 mg L^{-1}, respectively. Also shown are the control tests with 200 mg L^{-1} GO and only bacteria (two lines on the top of the figures). N_0 is the initial colony-forming units in water. N_t is the instant colony-forming units at time *t*. Results are expressed as mean ± SD of three repeated experiments.

3.2.2. pH

The effect of pH on the antibacterial activity was displayed in Fig. 4. It was found that GO-Ag showed a better antibacterial activity against both *E. coli* and *S. aureus* bacteria under acidic condition in comparison to the disinfection of the same water at higher pH value. For *E. coli*, the antibacterial rates were 81.68%, 75.5% and 70.5%, and for *S. aureus*, the antibacterial rates were 58.23%, 45.96% and 40.6%, when the pH values were 5.5, 7 and 8.5, respectively. This result could be explained by the different concentrations of silver ions released from AgNPs at varying pH values [36]. It has been proposed that ionic silver is the effective speciation to directly damage the bacteria [37]. In aqueous solutions, AgNPs may be oxidized into silver ion by dissolved oxygen, which could be expressed by the following equation [38]:

$$4Ag_{(s)} + O_{2(aq)} + 4H^{+} = 4Ag^{+}_{(aq)} + 2H_2O_{(l)} \quad (4)$$

It is obvious that the amount of silver ions released from GO-Ag depends on the extent of AgNPs oxidation which is significantly influenced by the hydrogen ion concentration. Therefore, lower pH resulted in more rapid release of silver ions and higher antibacterial activity.

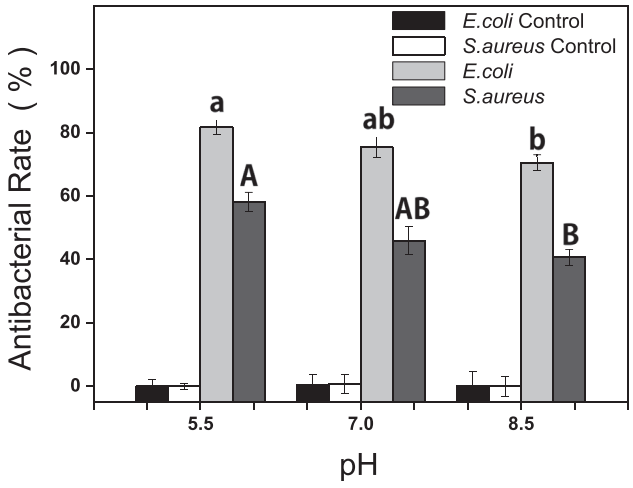

Fig. 4. Effect of pH on antibacterial activity using 200 mg L^{-1} bactericide under acidic (pH = 5.5), neutral (pH = 7) and alkaline (pH = 8.5) conditions. Results are expressed as mean ± SD of three independent experiments. Different letters denote statistically significant differences ($P < 0.05$) between bars of the experimental group.

3.3. Antibacterial mechanism studies

3.3.1. Interaction between bacterial cells and antibacterial materials

The observation of bacterial cells morphology is helpful for the evaluation of antibacterial activity and the exploration of antibacterial mechanism after being exposed to nanomaterials [15]. Fig. 5 showed the results of SEM illustrating the property and degree of cells damage. The native *E. coli* exhibited a typically baculiform shape and the whole cell was encircled by extracellular secretion separated itself from the external environment (Fig. 5a). After being exposed to GO-Ag, the cell body of *E. coli* was badly damaged and the cell debris mixed with the extracellular secretion (Fig. 5b). As for *S. aureus*, the native cell was globular (Fig. 5c) and was easy to be recognized under SEM. Nevertheless, the treated *S. aureus* swelled up and deformed into an elongated shape (Fig. 5d). For both treated *E. coli* and treated *S. aureus*, there were eight out of ten cells that showed such phenotypes at least, and representative cell images of GO-Ag treated *E. coli* and *S. aureus* are selected and showed in Fig. 5 b and d. Additionally, GO-Ag was much more destructive to cell membrane of *E. coli* than that of *S. aureus*, which could also provide evidence for the aforementioned result that antibacterial activity of GO-Ag against *E. coli* was more effective.

Cell membranes were the first to be affected when the cells were exposed to harmful material. Positively charged silver ions were easily taken up by negatively charged lipids on cell membranes because of electrostatic attraction. Silver ions interacted with membrane proteins or phospholipid bilayer resulting in the increase of membrane permeability [39,40]. It is well known that the selective permeability of cell membrane controls the substances passing in and out. As a result, intracellular contents leaked out and extracellular substances leaked in, causing the change of cells morphology and finally death [41].

3.3.2. Identification of bactericidal species

For the purpose of identifying the bactericidal species, the influence of two antioxidant enzymes (CAT and SOD) and a silver ions neutralizer (NATG) on antibacterial activity were explored. The results were illustrated in Fig. 6. The main function of SOD is accelerating the disproportionation of superoxide anion radical to form hydrogen peroxide and molecular oxygen (Eq. (6)), while CAT

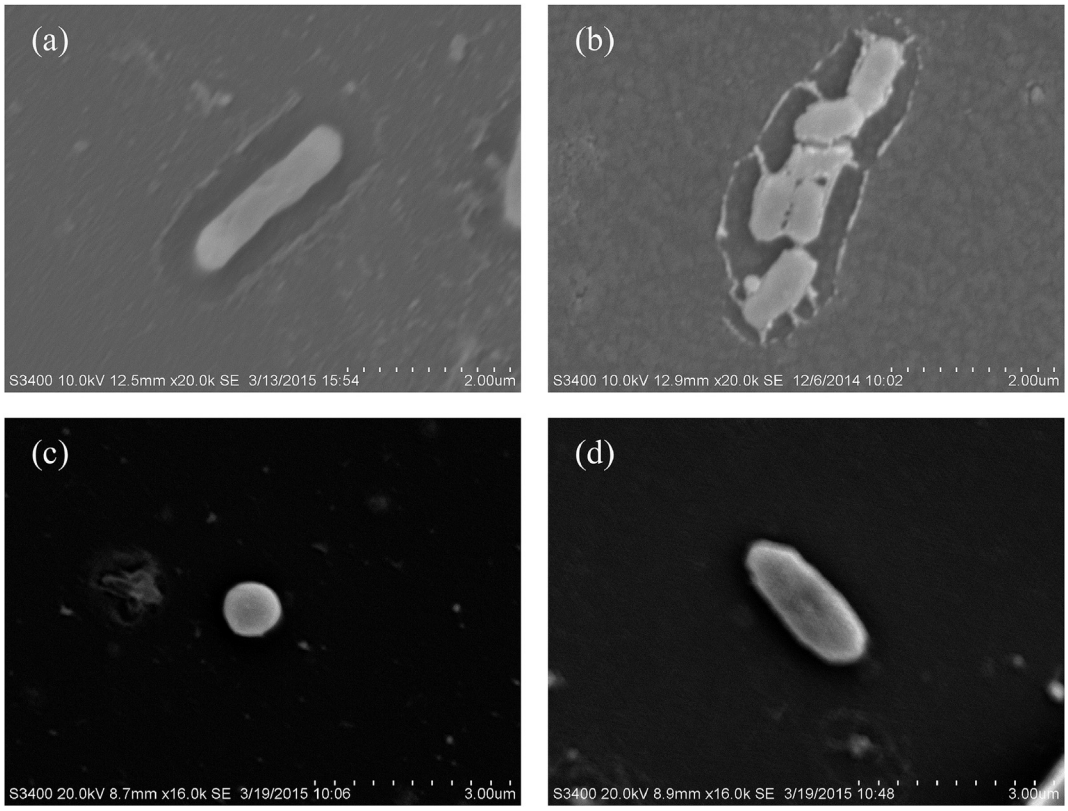

Fig. 5. SEM images of native *E. coli* (a), treated *E. coli* (b), native *S. aureus* (c) and treated *S. aureus* (d).

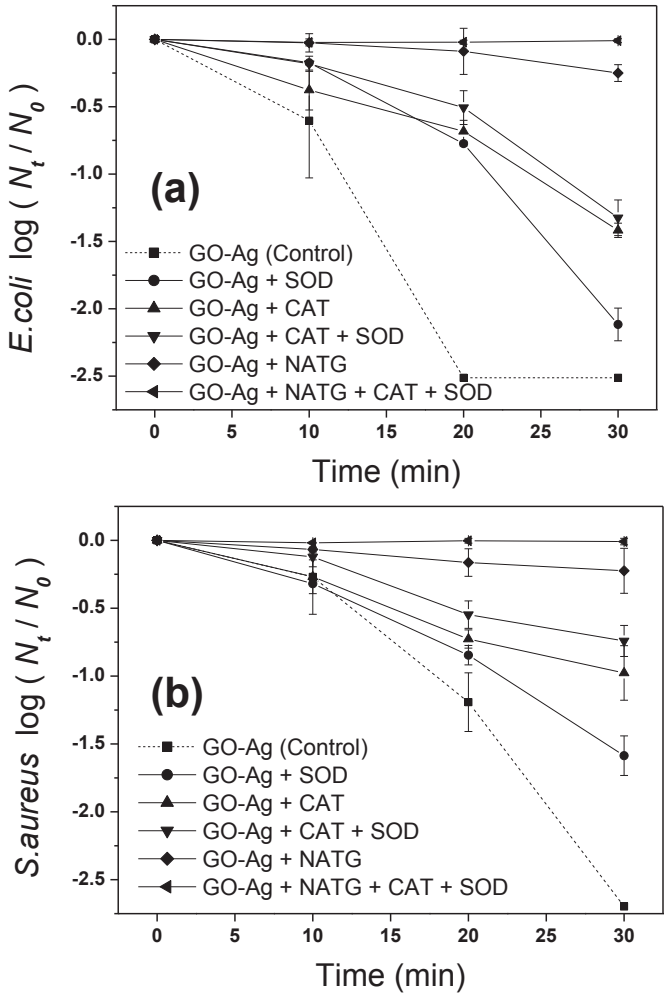

Fig. 6. Effect of CAT, SOD and NATG on antibacterial activity against *E. coli* (a) and *S. aureus* (b). CAT, SOD and NATG were added to 0.1% w/v, respectively. The concentrations of GO-Ag were 200 mg L^{-1}. Also shown is the control with only addition of GO-Ag (dashed line). N_0 is the initial colony-forming units in water. N_t is the instant colony-forming units at time *t*. Representative results of one of three independent experiments are shown.

can catalyze the process of converting hydrogen peroxide into water and molecular oxygen (Eq. (7)). And the NATG was used to neutralize silver ions in the aqueous. Compared with the control, there was an obvious inhibition of antibacterial effects in presence of CAT, SOD and NATG. For *S. aureus* species, the antibacterial rate reached 99.80% without scavenger or neutralizer. When SOD, CAT and NATG were added separately, the antibacterial rates decreased to 97.41%, 89.45% and 40.33%, respectively. And the antibacterial effect almost completely inhibited with a synergy effect of the three additional agents. Similar consequence was observed in the antibacterial tests against *E. coli*. These results indicated that the formation of silver ions, superoxide anion radical and hydrogen peroxide contributed to the antibacterial activity.

$$2\cdot O_2^- + 2H^+ \xrightarrow{SOD} H_2O_2 + O_2 \quad (5)$$

$$2H_2O_2 \xrightarrow{CAT} 2H_2O + O_2 \quad (6)$$

Many studies have reported that AgNPs can kill bacterial cells by damaging the cell membranes and causing the loss of cellular integrity [21,41]. However, based on the results in Fig. 6, AgNPs loaded on the GO sheets had to first form silver ions to disinfect the water. When the silver ions in aqueous solutions were neutralized, the antibacterial rates dropped sharply. These results further confirmed that silver ions were the key substance to directly kill bacteria.

It is inevitable that silver ions interact with intracellular enzymes after they pass across cell membrane. The interaction of silver ions with enzymes of the respiratory chain can result in leakage of electrons during the process they passed through the mitochondrial electron transport chain. Then, superoxide is formed with molecular oxygen as electron acceptor [42–44]. By the catalysis of SOD, superoxide produces hydrogen peroxide, which can be fully reduced to water or partially reduced to a stronger oxidant, hydroxyl radical. Superoxide anion radical, hydrogen peroxide and hydroxyl radical are the main ROS in cells. High concentration of ROS may react with various biomacromolecules, causing irreversibly oxidative damage such as denaturation, fracture and crosslinking and eventually leading to death. In our tests, the addition of SOD and CAT decreased the bactericidal effect against both Gram-negative and Gram-positive bacteria, which suggested that the generation of superoxide anion radical and hydrogen peroxide accounted for the antibacterial activity of GO-Ag.

3.3.3. Oxidative stress induced by GO-Ag

To further probe the potential role of oxidative stress in antibacterial behavior of GO-Ag, total superoxide dismutase (T-SOD) and CAT activity in *E. coli* and *S. aureus* were measured. The main antioxidant enzymes generated intracellularly, including SOD and CAT, can eliminate ROS and prevent polyunsaturated fatty acids (PUFA) in biomembranes from lipid peroxidation. Under natural conditions, the generation and elimination of ROS at an extremely low and hurtless level are in dynamic equilibrium. Once the content of ROS generated was out of the clearing range, the equilibrium would be broken. The changes of intracellular T-SOD and CAT activity were shown in Fig. 7. After exposed to GO-Ag for 20 min, the T-SOD activity in *E. coli* and *S. aureus* increased to 1.33 and 1.36 times (Fig. 7a) of that in native cells, while the CAT activity in *E. coli* and *S. aureus* were 4 and 9 times (Fig. 7b) more compared with the control group ($P < 0.05$), respectively. When ROS were produced in great numbers, bacterial cells would be stumilated to produce more antioxidants to intensify the defense system for eliminating redundant ROS and reducing oxidative damage [45]. Therefore, the enhancement of antioxidants indicated that bacterial cells were in the state of oxidative stress during the antibacterial process.

The excessive ROS are easy to cause lipid peroxidation which is extensively used for toxicity detection of nanomaterials towards cells. Hydroxyl radical induced by GO-Ag could snatch hydrogen atom form allylic position of the PUFA to form allyl free radical. Then, the product might react with molecular oxygen to create lipid peroxide radical which could rearrange to form MDA [46]. Many researches also pointed that the generation of MDA was caused by PUFA peroxidation, and the content of MDA was in relation to the ROS concentration [46–48]. Therefore, the detection of MDA could reflect the situation of lipid peroxidation and the extent of cells oxidative damage indirectly. As illustrated in Fig. 7c, there were few MDA presented in native cells, however, the contents of MDA increased sharply after exposed (17.5 times for *E. coli* and 15 times for *S. aureus*), which showed that the bacteria underwent severe oxidative stress caused by a lot of ROS during the bactericidal process of GO-Ag.

3.3.4. Antibacterial mechanism of GO-Ag

According to the results above, the whole process of GO-Ag nanocomposites disinfection includes multiple stages (Fig. 8). The

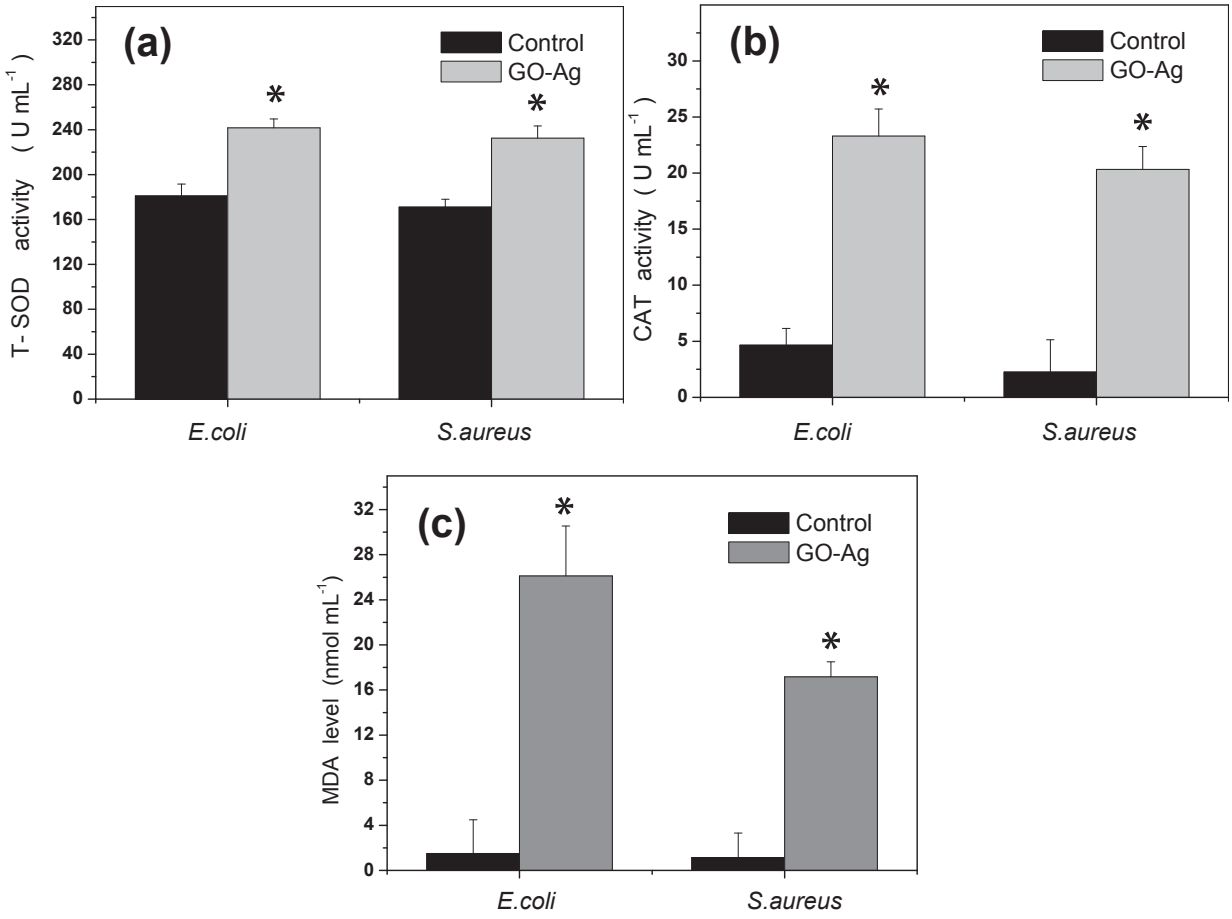

Fig. 7. The changes of intracellular T-SOD (a), CAT (b) activity and content of MDA (c) in cells after exposure to GO-Ag for 20 min compared with the control. Three independent assays were performed and the results are expressed as the mean ± S.D. Statistical differences ($P < 0.05$) from the control are marked with asterisk.

first stage is the oxidation of AgNPs loaded on the GO sheets by dissolved oxygen. At this stage, GO-Ag nanocomposites can be dispersed into water to form stable aqueous colloids due to the good hydrophilic affinity and aqueous dispersibility of GO sheets [49]. The parameters of oxidative process such as pH, dissolved oxygen concentration [36,50,51], undoubtedly affect the final efficiency of disinfection. The second stage involves the contact between free silver ions and bacterial cells. In this stage, electrostatic attraction plays an important role because negatively charged lipids on cell membranes are easy to capture positively charged silver ions [39,52]. Since silver ions directly interact with bacterial cells, the substances which can precipitate or neutralize silver ions are likely to block this process. This can be confirmed by the experimental results above. In our tests, the antibacterial rates were sharply decreased with the addition of silver ions neutralizer. The third stage is that silver ions make disruptive interaction with bacteria through binding membrane proteins or phospholipid bilayer. After the destruction of membrane system, a large number of free silver ions, even GO-Ag nanocomposites, can enter into the cells [53]. SEM images in Fig. 5 show the disruption role of GO-Ag. The final stage involves the interference via silver ions directly binding with proteins, lipids, enzymes, DNA and the oxidation of them by generating ROS [54]. The generation of ROS and oxidative stress are more significant mechanism owing to the strong destructive power. As illustrated in Fig. 8, ROS were mainly generated by the mitochondrial electron transport chain. Excessive ROS production can lead to oxidation of proteins, lipids, and DNA. The peroxidation of membrane lipid causes the damage of cell membrane, leading to generation of MDA and leakage of cell content [55,56]. The oxidation of intracellular biomacromolecules causes irreversible damage, and eventually cell death. According to the results above, synergetic mechanism including destruction of cell membranes and oxidative stress accounted for the antibacterial activity of GO-Ag nanocomposites.

4. Conclusions

In this work, GO-Ag nanocomposites exhibiting great antibacterial activity in aqueous solutions were successfully prepared. The effects of bactericide dosage and pH on the antibacterial activity and antibacterial mechanism were discussed. Antibacterial behavior of GO-Ag against both bacterial strains was dose and contact time dependent, and the antibacterial activity was more effective against *E. coli* than *S. aureus*. Under lower pH value condition, GO-Ag exhibited a more effective antibacterial activity in aqueous solutions. SEM images of bacteria showed that GO-Ag was much more destructive to cell membrane of *E. coli* than that of *S. aureus*. Silver ions were the key substance to directly kill bacteria, while AgNPs loaded on the GO sheets had to first be oxidized into silver ions. The formation of superoxide anion radical and hydrogen peroxide contributed to the antibacterial activity. The intracellular antioxidant enzymes and content of MDA sharply increased after the bacteria were exposed to GO-Ag. Synergetic mechanism including destruction of cell membranes and

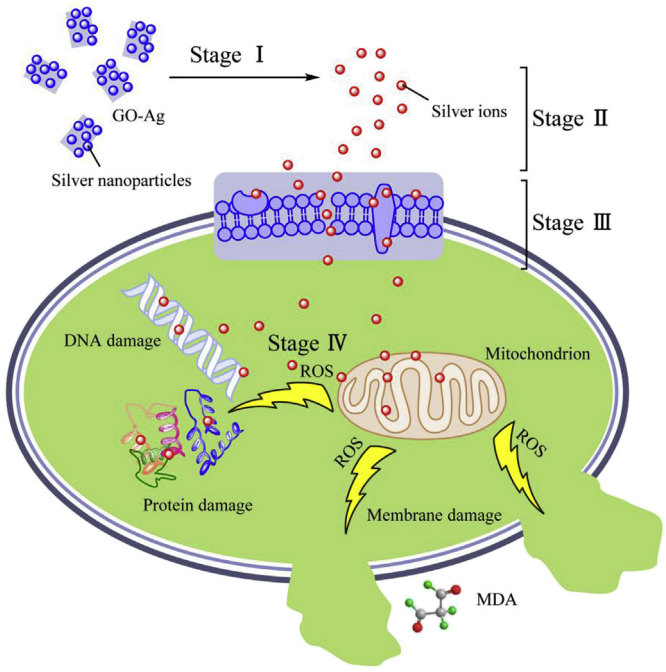

Fig. 8. Schematic mechanisms for antibacterial behaviors of GO-Ag. Blue dots represent silver nanoparticles loaded on GO sheets, and red dots are silver ions. The roman numerals (I, II, III, and IV) refer to different stages of the bactericidal process. (For interpretation of the references to colour in this figure legend, the reader is referred to the web version of this article.)

oxidative stress accounted for the antibacterial activity of GO-Ag nanocomposites. However, it remains unknown whether the bactericides leads to drug resistance of pathogenic bacteria after longtime usage. And the separation of bactericides after disinfection needs further investigation. The higher production costs of GO-Ag nanocomposites compared with conventional disinfectants is also a drawback. Despite these disadvantages, the as-prepared bactericides showed a good potential for application in water disinfection.

Acknowledgements

The authors are grateful for the financial supports from National Natural Science Foundation of China (51521006, 51579095, 51378190), the Program for Changjiang Scholars and Innovative Research Team in University (IRT-13R17), Hunan province university innovation platform open fund project (14K020) and the Interdisciplinary Research Funds for Hunan University.

References

[1] G.P. Winward, L.M. Avery, T. Stephenson, B. Jefferson, Chlorine disinfection of grey water for reuse: effect of organics and particles, Water Res. 42 (2008) 483–491.
[2] C.J. Volk, R. Hofmann, G. Ranger, R.C. Andrews, C. Chauret, G.A. Gagnon, Implementation of chlorine dioxide disinfection: effects of the treatment change on drinking water quality in a full-scale distribution system, J. Environ. Eng. Sci. 1 (2002) 323–330.
[3] P. Xu, M.L. Janex, P. Savoye, A. Cockx, V. Lazarova, Wastewater disinfection by ozone: main parameters for process design, Water Res. 36 (2002) 1043–1055.
[4] W. Lee, P. Westerhoff, Formation of organic chloramines during water disinfection-chlorination versus chloramination, Water Res. 43 (2009) 2233–2239.
[5] S.D. Richardson, C. Postigo, Drinking water disinfection by-products, in: D. Barceló (Ed.), Emerging Organic Contaminants and Human Health, Springer Berlin Heidelberg, Berlin, Heidelberg, 2012, pp. 93–137.
[6] J.J. Rook, Formation of haloforms during chlorination of natural waters, Water Treat. Exam. 23 (1974) 234–243.
[7] S.W. Krasner, H.S. Weinberg, S.D. Richardson, S.J. Pastor, R. Chinn, M.J. Sclimenti, G.D. Onstad, A.D. Thruston Jr., Occurrence of a new generation of disinfection byproducts, Environ. Sci. Technol. 40 (2006) 7175–7185.
[8] S.D. Richardson, A.D. Thruston Jr., C. Rav-Acha, L. Groisman, I. Popilevsky, O. Juraev, V. Glezer, A.B. Mckague, M.J. Plewa, E.D. Wagner, Tribromopyrrole, brominated acids, and other disinfection byproducts produced by disinfection of drinking water rich in bromide, Environ. Sci. Technol. 37 (2003) 3782–3793.
[9] C.Y. Chang, Y.H. Hsieh, S.S. Hsu, P.Y. Hu, K.H. Wang, The formation of disinfection by-products in water treated with chlorine dioxide, J. Hazard. Mater. 79 (2000) 89–102.
[10] S.S. Birla, V.V. Tiwari, A.K. Gade, A.P. Ingle, A.P. Yadav, M.K. Rai, Fabrication of silver nanoparticles by Phoma glomerata and its combined effect against *Escherichia coli*, *Pseudomonas aeruginosa* and *Staphylococcus aureus*, Lett. Appl. Microbiol. 48 (2009) 173–179.
[11] K.J. Kim, W.S. Sung, B.K. Suh, S.K. Moon, J.S. Choi, J.G. Kim, D.G. Lee, Antifungal activity and mode of action of silver nano-particles on *Candida albicans*, Biometals 22 (2009) 235–242.
[12] M. Rai, A. Yadav, A. Gade, Silver nanoparticles as a new generation of antimicrobials, Biotechnol. Adv. 27 (2009) 76–83.
[13] Y. Zhu, S. Murali, W. Cai, X. Li, J.W. Suk, J.R. Potts, R.S. Ruoff, Graphene and graphene oxide: synthesis, properties, and applications, Adv. Mater. 22 (2010) 3906–3924.
[14] S. Gurunathan, J.W. Han, A.A. Dayem, V. Eppakayala, J.H. Kim, Oxidative stress-mediated antibacterial activity of graphene oxide and reduced graphene oxide in *Pseudomonas aeruginosa*, Int. J. Nanomed. 7 (2012) 5901–5914.
[15] S. Liu, T.H. Zeng, M. Hofmann, E. Burcombe, J. Wei, R. Jiang, K. Jing, C. Yuan, Antibacterial activity of graphite, graphite oxide, graphene oxide, and reduced graphene oxide: membrane and oxidative stress, Acs Nano 5 (2011) 6971–6980.
[16] J.D. Kim, H. Yun, G.C. Kim, C.W. Lee, H.C. Choi, Antibacterial activity and reusability of CNT-Ag and GO-Ag nanocomposites, Appl. Surf. Sci. 283 (2013) 227–233.
[17] O.N. Ruiz, N.A. Brown, K.A. Shiral Fernando, B.A. Harruff-Miller, T.S. Gunasekera, C.E. Bunker, Graphene oxide-based nanofilters efficiently remove bacteria from fuel, Int. Biodeterior. Biodegr. 97 (2015) 168–178.
[18] A.F. de Faria, D.S.T. Martinez, S.M.M. Meira, A.C.M. de Moraes, A. Brandelli, A.G.S. Filho, O.L. Alves, Anti-adhesion and antibacterial activity of silver nanoparticles supported on graphene oxide sheets, Colloids Surf. B. Biointerfaces 113 (2014) 115–124.
[19] G. Xiao, X. Zhang, W. Zhang, S. Zhang, H. Su, T. Tan, Visible-light-mediated synergistic photocatalytic antimicrobial effects and mechanism of Ag-nanoparticles@chitosan-TiO_2 organic-inorganic composites for water disinfection, Appl. Catal. B Environ. 170–171 (2015) 255–262.
[20] A. Khalil, M.A. Gondal, M.A. Dastageer, Augmented photocatalytic activity of palladium incorporated ZnO nanoparticles in the disinfection of *Escherichia coli* microorganism from water, Appl. Catal. A Gen. 402 (2011) 162–167.
[21] T. Parandhaman, A. Das, B. Ramalingam, D. Samanta, T.P. Sastry, A.B. Mandal, S.K. Das, Antimicrobial behavior of biosynthesized silica-silver nanocomposite for water disinfection: a mechanistic perspective, J. Hazard. Mater. 290 (2015) 117–126.
[22] A.S. Pina, I.L. Batalha, C.S. Fernandes, M.A. Aoki, A.C. Roque, Exploring the potential of magnetic antimicrobial agents for water disinfection, Water Res. 66 (2014) 160–168.
[23] W.S. Hummers, R.E. Offeman, Preparation of graphitic oxide, J. Am. Chem. Soc. 80 (1958) 1339.
[24] C.H. Deng, J.L. Gong, G.M. Zeng, C.G. Niu, Q.Y. Niu, W. Zhang, H.Y. Liu, Inactivation performance and mechanism of *Escherichia coli* in aqueous system exposed to iron oxide loaded graphene nanocomposites, J. Hazard. Mater. 276 (2014) 66–76.
[25] H.I. Won, H. Nersisyan, C.W. Won, J.M. Lee, J.S. Hwang, Preparation of porous silver particles using ammonium formate and its formation mechanism, Chem. Eng. J. 156 (2010) 459–464.
[26] X. Zou, J. Shi, H. Zhang, Coexistence of silver and titanium dioxide nanoparticles: enhancing or reducing environmental risks? Aquat. Toxicol. 154 (2014) 168–175.
[27] H. Ukeda, S. Maeda, T. Ishii, M. Sawamura, Spectrophotometric assay for superoxide dismutase based on tetrazolium salt 3′-1-(phenylamino)-carbonyl-3, 4-tetrazolium]-bis(4-methoxy-6-nitro)benzenesulfonic acid hydrate reduction by xanthine-xanthine oxidase, Anal. Biochem. 251 (1997) 206–209.
[28] L. Góth, A simple method for determination of serum catalase activity and revision of reference range, Clin. Chim. Acta 196 (1991) 143–151.
[29] D. Ali, P.G. Yadav, S. Kumar, H. Ali, S. Alarifi, A.H. Harrath, Sensitivity of freshwater pulmonate snail *Lymnaea luteola* L., to silver nanoparticles, Chemosphere 104 (2014) 134–140.
[30] Y. Lai, H. Zhuang, K. Xie, D. Gong, Y. Tang, L. Sun, C. Lin, Z. Chen, Fabrication of uniform Ag/TiO_2 nanotube array structures with enhanced photoelectrochemical performance, New J. Chem. 34 (2010) 1335–1340.
[31] Y. Liu, L. Fang, H. Lu, Y. Li, C. Hu, H. Yu, One-pot pyridine-assisted synthesis of visible-light-driven photocatalyst Ag/Ag_3PO_4, Appl. Catal. B Environ. 115–116 (2012) 245–252.
[32] Z. Zhu, M. Su, L. Ma, L. Ma, D. Liu, Z. Wang, Preparation of graphene oxide-silver nanoparticle nanohybrids with highly antibacterial capability, Talanta 117 (2013) 449–455.
[33] K.S. Hui, K.N. Hui, D.A. Dinh, C.H. Tsang, Y.R. Cho, W. Zhou, X. Hong, H. Chun,

Green synthesis of dimension-controlled silver nanoparticle-graphene oxide with in situ ultrasonication, Acta Mater. 64 (2014) 326–332.
[34] G. Giovannetti, P.A. Khomyakov, G. Brocks, V.M. Karpan, J.V.D. Brink, P.J. Kelly, Doping graphene with metal contacts, Phys. Rev. Lett. 101 (2008) 1676–1686.
[35] J.S. Kim, E. Kuk, K.N. Yu, J.H. Kim, S.J. Park, H.J. Lee, S.H. Kim, Y.K. Park, Y.H. Park, C.Y. Hwang, Y.K. Kim, Y.S. Lee, D.H. Jeong, M.H. Cho, Antimicrobial effects of silver nanoparticles, Nanomedicine 3 (2007) 95–101.
[36] W. Shao, H. Liu, X. Liu, H. Sun, S. Wang, R. Zhang, pH-responsive release behavior and anti-bacterial activity of bacterial cellulose-silver nanocomposites, Int. J. Biol. Macromol. 76 (2015) 209–217.
[37] D. Jiraroj, S. Tungasmita, D.N. Tungasmita, Silver ions and silver nanoparticles in zeolite A composites for antibacterial activity, Powder Technol. 264 (2014) 418–422.
[38] J. Liu, R.H. Hurt, Ion release kinetics and particle persistence in aqueous nano-silver colloids, Environ. Sci. Technol. 44 (2010) 2169–2175.
[39] G. Su, H. Zhou, Q. Mu, Y. Zhang, L. Li, P. Jiao, G. Jiang, B. Yan, Effective surface charge density determines the electrostatic attraction between nanoparticles and cells, J. Phys. Chem. C 116 (2012) 4993–4998.
[40] P. Dibrov, J. Dzioba, K.K. Gosink, C.C. Hase, Chemiosmotic mechanism of antimicrobial activity of Ag^{+} in vibrio cholerae, Antimicrob. Agents Chemother. 46 (2002) 2668–2670.
[41] I. Sondi, B. Salopek-Sondi, Silver nanoparticles as antimicrobial agent: a case study on *E. coli* as a model for Gram-negative bacteria, J. Colloid Interface Sci. 275 (2004) 177–182.
[42] K.B. Holt, A.J. Bard, Interaction of silver(I) ions with the respiratory chain of *Escherichia coli*: an electrochemical and scanning electrochemical microscopy study of the antimicrobial mechanism of micromolar Ag^{+}, Biochemistry 44 (2005) 13214–13223.
[43] J.F. Turrens, Mitochondrial formation of reactive oxygen species, J. Physiol. 552 (2003) 335–344.
[44] Y. Liu, G. Fiskum, D. Schubert, Generation of reactive oxygen species by the mitochondrial electron transport chain, J. Neurochem. 80 (2002) 780–787.
[45] V.I. Lushchak, Adaptive response to oxidative stress: bacteria, fungi, plants and animals, Comp. Biochem. Physiol. C Toxicol. Pharmacol. 153 (2011) 175–190.
[46] R.K. Dutta, B.P. Nenavathu, M.K. Gangishetty, A.V. Reddy, Studies on antibacterial activity of ZnO nanoparticles by ROS induced lipid peroxidation, Colloids Surf. B. Biointerfaces 94 (2012) 143–150.
[47] M. Ott, V. Gogvadze, S. Orrenius, B. Zhivotovsky, Mitochondria, oxidative stress and cell death, Apoptosis 12 (2007) 913–922.
[48] G. Ermak, K.J.A. Davies, Calcium and oxidative stress: from cell signaling to cell death, Mol. Immunol. 38 (2002) 713–721.
[49] S. Stankovich, D.A. Dikin, G.H. Dommett, K.M. Kohlhaas, E.J. Zimney, E.A. Stach, R.D. Piner, S.T. Nguyen, R.S. Ruoff, Graphene-based composite materials, Nature 442 (2006) 282–286.
[50] W. Zhang, Y. Yao, K. Li, Y. Huang, Y. Chen, Influence of dissolved oxygen on aggregation kinetics of citrate-coated silver nanoparticles, Environ. Pollut. 159 (2011) 3757–3762.
[51] E.K. Fauss, R.I. MacCuspie, V. Oyanedel-Craver, J.A. Smith, N.S. Swami, Disinfection action of electrostatic versus steric-stabilized silver nanoparticles on *E. coli* under different water chemistries, Colloids Surf. B. Biointerfaces 113 (2014) 77–84.
[52] W. Rathnayake, H. Ismail, A. Baharin, A. Darsanasiri, S. Rajapakse, Synthesis and characterization of nano silver based natural rubber latex foam for imparting antibacterial and anti-fungal properties, Polym. Test. 31 (2012) 586–592.
[53] Q.L. Feng, J. Wu, G.Q. Chen, F.Z. Cui, T.N. Kim, J.O. Kim, A mechanistic study of the antibacterial effect of silver ions on *Escherichia coli* and *Staphylococcus aureus*, J. Biomed. Mater. Res. 52 (2000) 662–668.
[54] C. Marambio-Jones, E.M.V. Hoek, A review of the antibacterial effects of silver nanomaterials and potential implications for human health and the environment, J. Nanopart. Res. 12 (2010) 1531–1551.
[55] E. Cadenas, K.J. Davies, Mitochondrial free radical generation, oxidative stress, and aging, Free Radic. Biol. Med. 29 (2000) 222–230.
[56] R.S. Balaban, S. Nemoto, T. Finkel, Mitochondria, oxidants, and aging, Cell 120 (2005) 483–495.